Effects of lanthanum modification on dielectric properties of Pb(Zr$_{0.90}$,Ti$_{0.10}$)O$_3$ ceramics: enhanced antiferroelectric stability

A. Peláiz-Barranco · J. D. S. Guerra · O. García-Zaldívar · F. Calderón-Piñar ·
E. B. Araújo · D. A. Hall · M. E. Mendoza · J. A. Eiras

Abstract Lanthanum modified lead zirconate titanate ceramics with lanthanum content changing from 2 to 6 at% La and a Zr/Ti ratio of 90/10 (PLZT x/90/10) have been analyzed by using X-ray diffraction, dielectric response, differential scanning calorimetry, and ferroelectric hysteresis. An antiferroelectric state was found to be stabilized, whereas the long-range ferroelectric state was disrupted by lanthanum substitution on the lead sites. A ferroelectric state is shown to be stable over an antiferroelectric state for low lanthanum contents in a wide temperature range, where both phases coexist. With the increase of the lanthanum concentration, the long-range coherency of the ferroelectric state is suppressed, i.e., the temperature range of the ferroelectric state stability decreased, disappearing for $x > 3$ at% La.

A. Peláiz-Barranco (✉) · O. García-Zaldívar ·
F. Calderón-Piñar
Facultad de Física-Instituto de Ciencia y Tecnología de Materiales, Universidad de La Habana, San Lázaro y L, Vedado., La Habana 10400, Cuba
e-mail: pelaiz@fisica.uh.cu

J. D. S. Guerra · E. B. Araújo
Departamento de Física e Química, Universidad Estadual Paulista, Ilha Solteira, SP 15385-000, Brazil

D. A. Hall
School of Materials, University of Manchester, Manchester M1 7HS, UK

M. E. Mendoza
Instituto de Física, Universidad Autónoma de Puebla. Apdo. Postal J-48, Puebla 72570, México

J. A. Eiras
Universidad Federal de São Carlos, Dpto. de Física, Rod. Wash. Luis, km. 235, São Carlos, SP 13.565-905, Brazil

Introduction

Materials with promissory characteristics for energy storage applications are those exhibiting antiferroelectric (AFE) behavior [1–3]. The AFE materials are commonly characterized by either a low dielectric permittivity with a field induced transition to a ferroelectric (FE) state at a critical electric field (named as threshold field), as in the case of the PbZrO$_3$ system [4, 5], or a relatively high dielectric permittivity, with a decreased electric field strength dependence, as in the case of the lanthanum modified lead zirconate titanate (PLZT) system [6, 7]. The phase transitions between the AFE and FE states have been traditionally considered as an object of intensive studies [7–9]. Recent investigations have led to the increasing interest in the study of such transitions and related phenomena because of the observed coexistence between the AFE and FE phases in perovskite structure-type materials [10–12]. The antiferroelectric-ferroelectric (AFE-FE) phase transition could occur spontaneously due to several factors, such as, a change in the stress configuration promoted by external mechanical driving fields, an increase in the amplitude of the applied ac electric field and/or by thermal changes. It is known that in ferroelectric systems the ferroelectric domains structure is characterized by a large spontaneous electrical polarization, whereas classical antiferroelectrics are frequently centrosymmetrics materials. Thus, a ferroelectric state can be induced in antiferroelectric systems with compositions near to the AFE-FE phase boundary (where both phases coexist) by applying high electric field levels. Otherwise, taking into account that antiferroelectric systems are more compact (from the atomic arrangement point of view), ferroelectric compositions close to the AFE-FE phase boundary can be transformed into antiferroelectric state by applying a hydrostatic pressure.

Lanthanum modified lead zirconate titanate (PLZT) has been found to show a dispersive behavior for both rhombohedral and tetragonal phases, as well as to increase the stability range of the antiferroelectric orthorhombic phase in the Zr-rich side of the phase diagram [13–15]. The corresponding phase diagram at room temperature shows regions where ferroelectric and antiferroelectric phases coexist, and thus both AFE and FE states must be similar free energy values. PLZT compositions close to the AFE-FE phase boundary are well-known systems because of the phase switching characteristic, that is to say, the electric field induced AFE-FE phase transformation takes place. The ability to switch between these two phases is related to the free energy of the crystal, whose value for AFE materials is comparable to that for the FE one because the free energy of the AFE crystal is comparable to that of the FE. The phase transformation is accompanied by a volume expansion and, therefore, the crystal structure is changed. The coexistence of the antiferroelectric and ferroelectric phases has been observed for the PLZT x/95/5 compositional sequence [16]. However, the antiferroelectric phase region of the PLZT compositional series has not yet been systematically investigated.

The aim of the present work is to study the effect of lanthanum modification on the antiferroelectric state of $Pb(Zr_{0.90},Ti_{0.10})O_3$ ferroelectric ceramics. The structural analysis by using X-ray diffraction shows that FE and AFE ordering coexist. The dielectric behavior and the hysteresis loops show the enhanced antiferroelectricity stability when the lanthanum content increases.

Experimental procedure

Ceramic samples were prepared by the traditional ceramic method [13] from nominal composition $(Pb_{1-x}La_x)$ $(Zr_{0.90}Ti_{0.10})_{1-x/4}O_3$, where $x = 2$, 3, 4, 5, and 6 at% La. The stoichiometric mixture of powders (PbO, ZrO_2, TiO_2, La_2O_3) was prefired at 800 °C in air for 1 h. The calcined powders were milled and conformed as thick disks by cold-pressing and sintering in air at 1250 °C for 1 h, in a well-covered platinum crucible in order to minimize the evaporation of reagents. The samples are hereafter labeled as PLZT x/90/10. X-ray diffraction analysis at room temperature was performed on powder samples by using a Rigaku Rotaflex RU200B diffractometer and CuK_α radiation. Electrodes were fabricated on the parallel faces by using Ag paste by a heat treatment at 590 °C. The dielectric properties were measured by using a HP4194A impedance analyzer in the temperature and frequency range of 40–300 °C and 100–10 MHz, respectively. The modulated differential scanning calorimetry (MDSC) analysis was made by using a MDSC 2920 TA instrument from room

temperature up to 350 °C and a temperature rate of 2.5 °C/min, with modulated amplitude of 1.5 °C during 50 s. Ferroelectric hysteresis loops were obtained by using a Sawyer-Tower circuit at 1 Hz and several temperatures.

Results

X-ray diffraction spectra results of the sintered PLZT x/90/10 ceramics are shown in Fig. 1. As can be seen, a pure PLZT perovskite phase structure with no additional secondary phases was observed for all the studied samples. A coexistence of the ferroelectric-rombohedral phase (R3m) and antiferroelectric-orthorhombic phases (Pbam) was obtained, which is in agreement with the phase diagram for the PLZT system [13]. As observed in Fig. 1 for the PLZT 2/90/10 composition, two additional rombohedral reflections [R (112), R (320)] appeared in the 2θ range of 36–55°, whereas the O (220) orthorhombic reflection was suppressed. The figure insets show the obtained behavior for the PLZT 2/90/10 and PLZT 3/90/10. The behavior observed around 55° in 2θ has not been shown because it is similar to that observed in the 2θ range of 37–38°. The
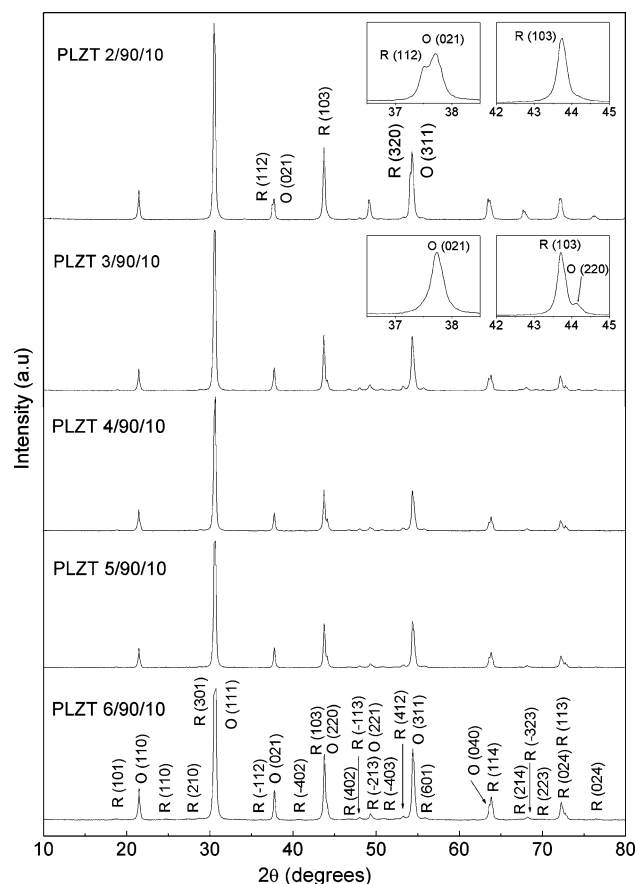

Fig. 1 X-ray diffraction pattern at room temperature for the PLZT x/90/10 studied compositions

PLZT 2/90/10 composition shows two reflections (R (320) and O (311)), while for PLZT compositions above 2 at% La only the O (311) reflection can be observed. Thus, the structural analysis has showed the contribution of two phases in the studied compositions, a ferroelectric-rombo-hedral phase and an antiferroelectric-orthorhombic phase. The PLZT 2/90/10 shows a higher contribution of the ferroelectric-romboedral phase than that for the PLZT compositions above 2 at% La.

The temperature dependence of the real dielectric permittivity (ε') for the PLZT x/90/10 compositional series is shown in Fig. 2, at several frequencies. As observed, no frequency dependence was observed for all the studied compositions within the investigated temperature range.

The obtained value for the paraelectric-ferroelectric phase transition temperature (T_m) for the PLZT 2/90/10 compo-sition was found to be around 201 °C, lower than that reported for the pure PZT 90/10 system [17]. On the other hand, an additional secondary dielectric anomaly was found for temperatures around 90 °C. The lower inset exhibits similar results for an expanded scale of tempera-tures (50–125 °C), and clearly shows a small anomalous behavior near 90 °C.

A further increment in the La content resulted in a continued suppression of the main dielectric peak (related to the PE-FE phase transition) and a decrement of T_m. As can be observed in the inserted figure (60–100 °C), the second anomaly still remains for the PLZT 3/90/10

Fig. 2 Temperature dependence of the real dielectric permittivity (ε') for the PLZT x/90/10 compositional series, at several frequencies
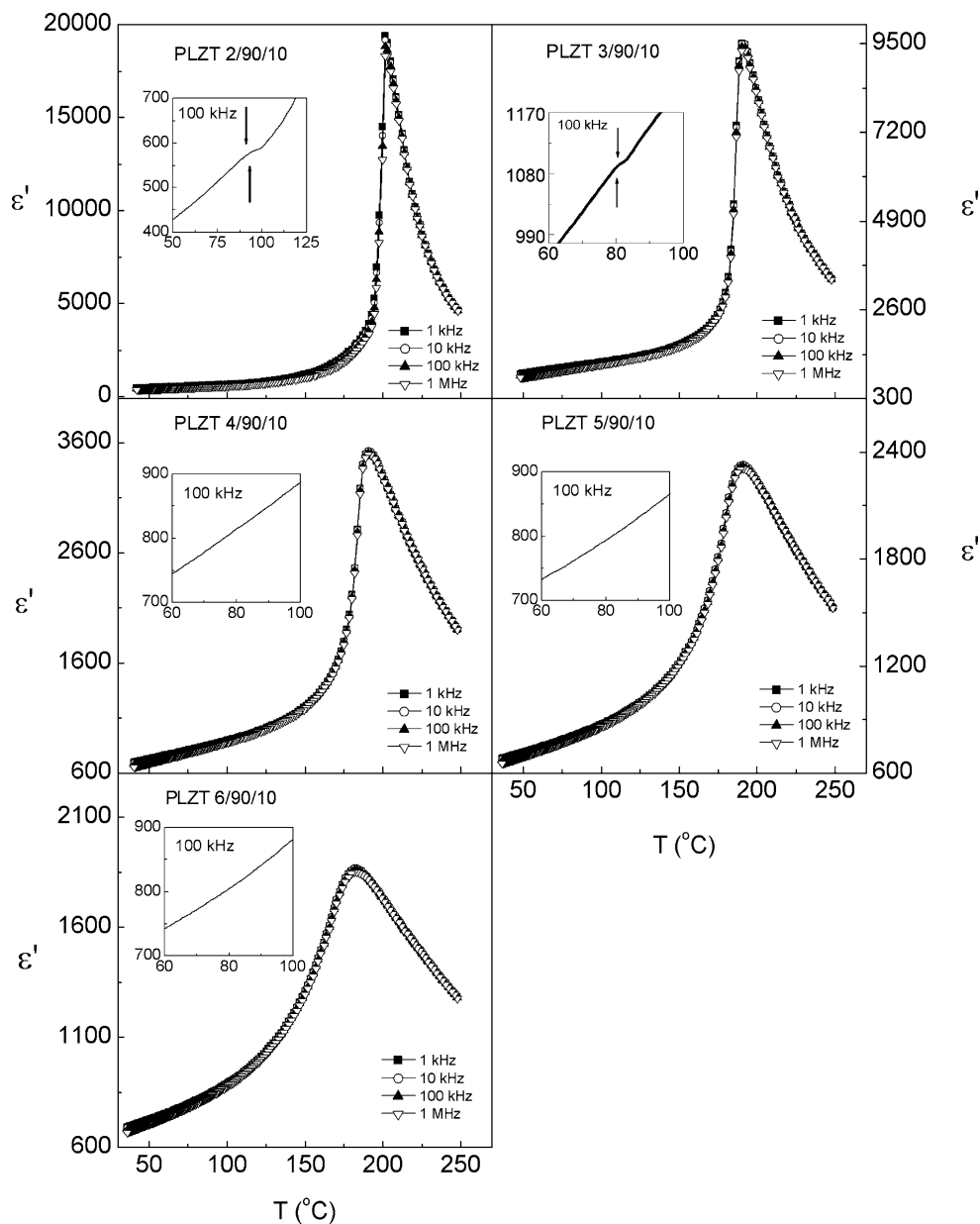
composition. For PLZT compositions above 3 at% La, this anomalous behavior completely disappeared (see the inset figures). On the other hand, the temperature-dependent dielectric response broadened in the compositional range between 4/90/10 and 6/90/10. For these samples the broad peaks for all the analyzed frequencies could suggests the existence of more than one contribution.

Figure 3 shows the temperature dependence of the imaginary part of the dielectric permittivity or losses factor (ε'') for the studied compositions at three selected frequencies. No frequency dependence was observed for the temperature corresponding to the maximum value of the losses factor ($T_{\varepsilon''max}$) within the investigated frequency range, showing similar values to that observed for the real

Table 1 Dielectric parameters for the studied PLZT x/90/10 compositions

Composition	T_m (°C)	ε'_{max}	$T_{\varepsilon'max}$ (°C)
PLZT 2/90/10	201	18779	200
PLZT 3/90/10	192	9408	191
PLZT 4/90/10	190	3508	186
PLZT 5/90/10	189	2316	186
PLZT 6/90/10	185	1854	179

part of the dielectric permittivity (T_m). Table 1 shows some of the obtained dielectric parameters for the studied samples. As observed, the difference between T_m and $T_{\varepsilon''max}$, in the dielectric response, increase for PLZT compositions

Fig. 3 Temperature dependence of the imaginary part of the dielectric permittivity (ε'') for the PLZT x/90/10 compositional series, at several frequencies
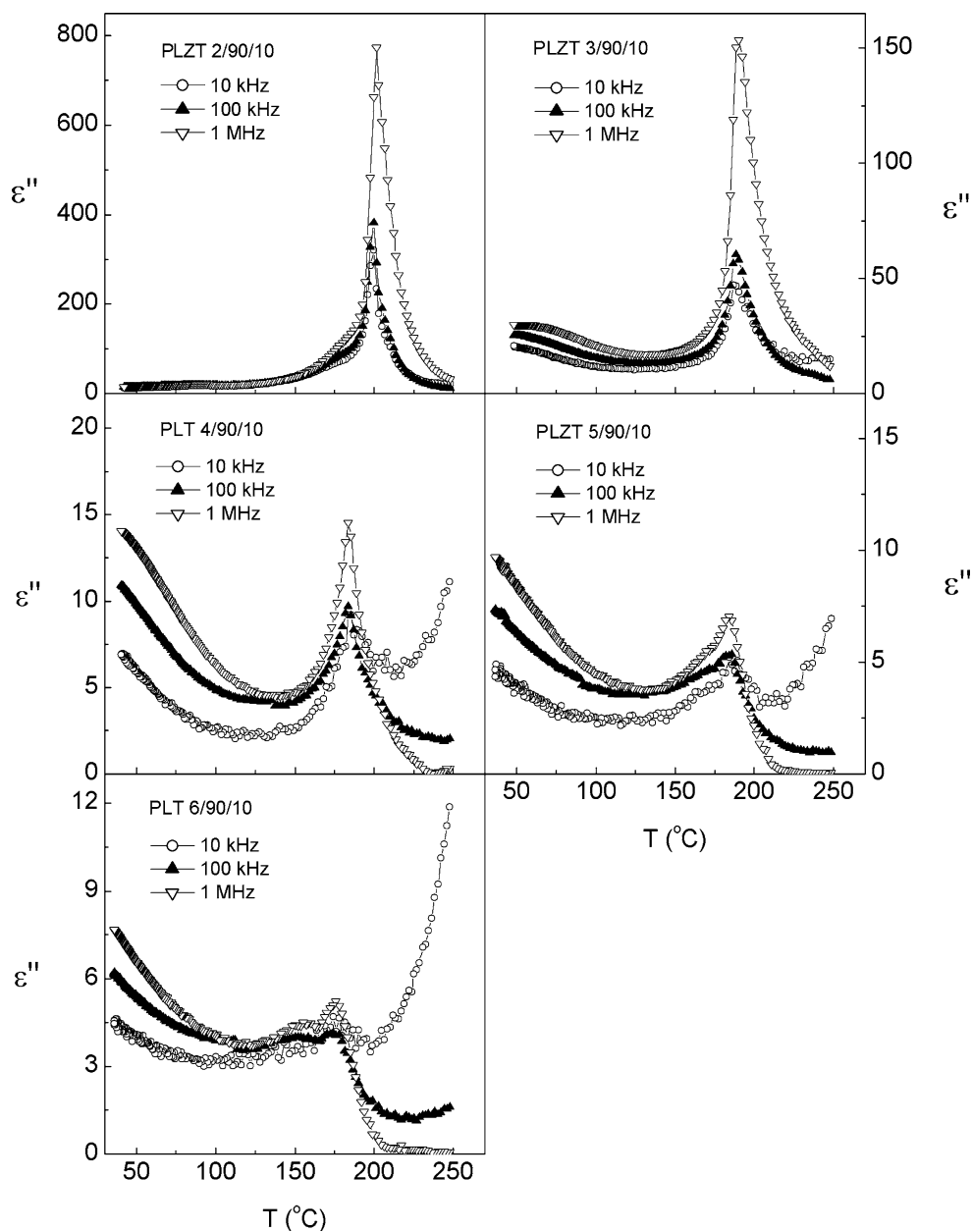
above 3 at% La, which could be associated to the broad-diffuse behavior observed for these compositions.

Thus, no evidence of relaxor-like dielectric response characteristics was observed in the PLZT x/90/10 samples. The PLZT 2/90/10 and PLZT 3/90/10 showed a secondary dielectric anomaly around 90 °C, as was observed in the temperature dependence of ε'.

Figure 4 shows the MDSC results for PLZT 2/90/10 and 3/90/10 compositions from room temperature up to 250 °C. The most pronounced dielectric anomaly for both samples occurs for temperatures around T_m, where C_P shows a sudden change. A small peak around 90 °C is observed for the PLZT 2/90/10 composition, corresponding to the anomalous behavior observed in the dielectric analysis results. For the PLZT 3/90/10 composition, even when only the peak associated to T_m is observed, a broad behavior was
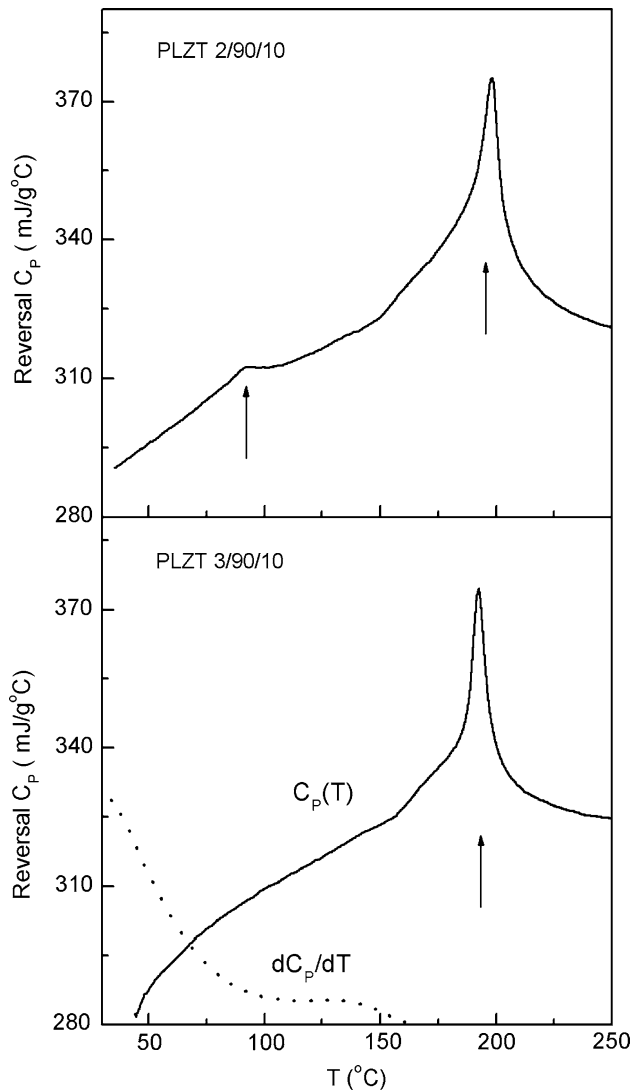
obtained in the temperature range where the second anomaly in the dielectric analysis (inset of Fig. 2) was observed. The derivative of the reversal C_P shows a clear inflexion around this temperature. However, for PLZT compositions above 3 at% La, only the peak associated to T_m was observed. Taking into account the structural, dielectric, and MDSC results, the observed second anomaly could be associated to either antiferroelectric-ferroelectric or ferroelectric-antiferroelectric phases transition.

In order to better identify the phases sequences, ferroelectric hysteresis loops were obtained at room temperature and 1 Hz, for the PLZT x/90/10 compositional series, as shown in Fig. 5. As can be seen, both the saturation and remanent polarizations (P_S and P_R, respectively) decrease with the increase of the lanthanum content. The decrease of the P_R parameter may reflect a decrease in the volume fraction of the ferroelectric state with the increase of the lanthanum content. For PLZT compositions above 3 at% La, slim loops were observed. For higher electric fields, typical characteristics of a field induced AFE-FE transition were obtained (see the inset figure for the PLZT 4/9010), although the saturation state could not be reached in the analyzed electric field range.

Figure 6 shows the temperature dependence of the ferroelectric properties for the studied PLZT x/90/10 compositions. Similar results were observed for PLZT 5/90/10 (not shown here) and PLZT 6/90/10 compositions. For the PLZT 2/90/10 composition, the values of P_R, P_S, and the coercive field (E_C) decrease with the increase of the temperature. These results suggest that the sample behave as typical ferroelectric system in the studied temperature range. It is interesting to note that the ferroelectric hysteresis loops did not show any anomalous behavior for temperatures around 90 °C, where a secondary dielectric anomaly was previously observed by the dielectric measurements. A small volume fraction of antiferroelectric phase coexists with the ferroelectric state as revealed by the X-ray analysis, although its contribution is lower than that for the ferroelectric phase. For the PLZT 3/90/10 composition, typical features of a field-induced AFE-FE transition
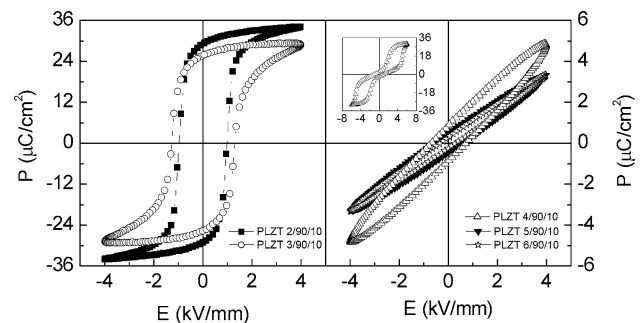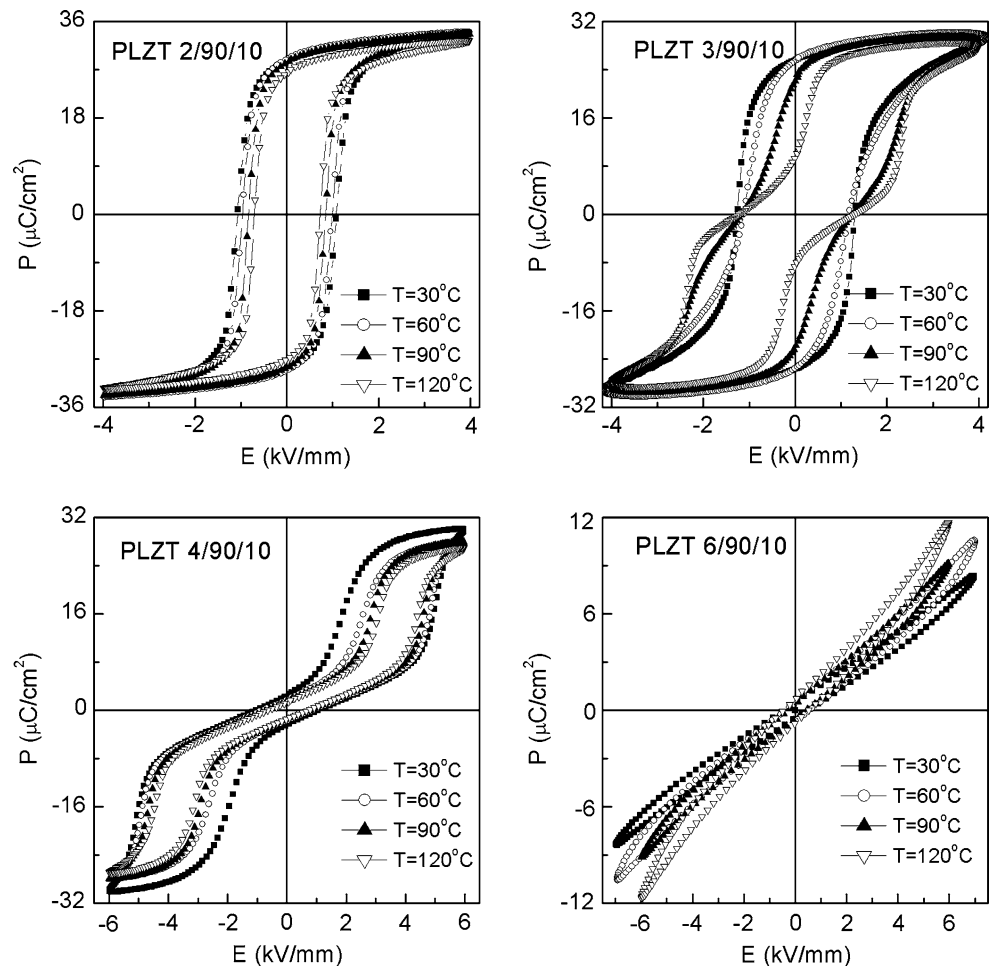

Fig. 4 MDSC results for the PLZT 2/90/10 and 3/90/10 compositions, from room temperature up to 250 °C

Fig. 5 Hysteresis loops obtained at room temperature for the PLZT x/90/10 studied compositions

Fig. 6 Hysteresis loops for the PLZT x/90/10 (x = 2, 3, 4, 6 at% La), as a function of the temperature

can be observed with the increase of the temperature, which indeed becomes more intense for temperatures above 90 °C. For PLZT composition above 3 at% La, the switching field for the AFE-FE phase transition is determined to be temperature dependent. Furthermore, no evidence or relaxor-like dielectric response characteristics were observed in the PLZT x/90/10 compositional sequence. Thus, rather than establishing a polar nanodomain state, the lanthanum modification resulted in the destabilization of the rombohebral ferroelectric state, leading to the stabilization of an antiferroelectric state.

From the dielectric, calorimetric, ferroelectric, and structural studies it could be concluded that the phase sequence with the increase of the temperature, for the PLZT 2/90/10 composition, can be considered as (i) a coexistence of the AFE and FE states at room temperature with no stabilization of the AFE phase, (ii) an AFE-FE phase transition around 90 °C, and (iii) a transition to the paraelectric phase at T_m. At the same time, for the PLZT 3/90/10 composition, these phase sequences can be considered as (i) a coexistence of the AFE and FE states at room temperature with no stabilization of the AFE phase, (ii) a stabilization of the AFE state for temperatures around

90 °C, and (iii) the transition to the paraelectric state at T_m. Otherwise, for PLZT compositions above 3 at% La, a coexistence between the AFE and FE states at room temperature can be observed with the stabilization of the AFE phase over the FE phase. The transition from the antiferroelectric to the paraelectric phase prevails at T_m, which is very far from room temperature.

Discussion

It is known that in lanthanum modified PZT materials, most of the lanthanum ions locate into the A-sites of the perovskite structure, replacing the lead cations [13]. The perovskite structure (ABO$_3$) can be considered as a network of BO$_6$ octahedron, where the B- and the A-site cations are located inside and in the neighboring of the octahedral, respectively [13]. The stability of the long-range ferroelectric state is believed to be suppressed by decoupling effects caused by the incorporation of lanthanum ions into the A-sites, which is revealed by the decreasing of the ferroelectric-paraelectric transition temperature, when the lanthanum concentration increases. The obtained results in the present work have clearly shown the

suppression of the stability of the ferroelectric state with a further enhancement of the antiferroelectric state with the increase of the lanthanum content.

It is known that the ferroelectricity phenomenon results from long-range Coulomb interactions between dipole moments, which can be described by the condensation of a transverse optical phonon mode at the center of Brillouin zone following lattice dynamics [13]. On the other hand, the antiferroelectric state results from a condensing of a transverse optical phonon mode at the boundary of the Brillouin zone, resulting from short-range interactions between atomic dipole moments. By considering that the addition of small lanthanum concentrations leads to decrease in the long-range interactions, reducing the stability of the ferroelectric phase, it is expected a reduction of the observed "average" T_m value. However, it would be very difficult for small concentration of the additive cation to suppress the short-range nature of the interactions in the antiferroelectric state. Thus, for the studied samples, lanthanum impurities may induce a competition between the antiferroelectric and ferroelectric ordering due to the disruption of long-range dipolar interactions. A ferroelectric state is shown to be more stable for low lanthanum contents at room temperature (as in the case of the PLZT 2/90/10 and 3/90/10 compositions). Both phases (AFE and FE) coexist over a relatively wide temperature range (from room temperature up to around 90 °C), showing a stable ferroelectric state, with low contribution of the AFE one. The disruption of the long-range dipolar interactions by 2 at% lanthanum doping is not enough to destabilize the ferroelectric state with respect to the antiferroelectric in the studied temperature range. For PLZT 3/90/10 composition, for temperatures around 90 °C, the long-range ordering of the ferroelectric state is suppressed by an excess of the lanthanum content in the perovskite structure. With the increase of the lanthanum concentration, the temperature range of the ferroelectric state stability decreased, disappearing for $x > 3$ at% La, that is to say, the antiferroelectric state becomes a more stable phase than the ferroelectric one, for temperatures above the room temperature. The rhombohedral ferroelectric PZT ceramics, which are close to the antiferroelectric-ferroelectric (AFE-FE) phase boundary, show that the FE phase is only marginally stable with respect to the AFE state. When the FE state is disrupted by lanthanum modification, the AFE state is stabilized.

Conclusions

In summary, the investigations of PLZT ceramics with the x/90/10 ($x = 2$, 3, 4, 5, and 6 at% La) using X-ray diffraction, dielectric behavior, differential scanning calorimetry, and ferroelectric measurements have clearly shown that the lanthanum modification of the PZT (Zr/Ti = 90/10) system disrupts the long-range dipolar order of the ferroelectric state, stabilizing an antiferroelectric state. For lower lanthanum contents (2 at% La), a ferroelectric state is shown to be stable with respect to the antiferroelectric state, for a wide temperature range. With the increase of the lanthanum concentration, the temperature range for the stability of the ferroelectric state decreased, disappearing for PLZT compositions above 3 at% La.

References

1. Jaffe B (1961) Proc IRE 49:1264
2. Pan W, Zhang Q, Bhalla A, Cross LE (1989) J Am Ceram Soc 72:571. doi:10.1111/j.1151-2916.1989.tb06177.x
3. Kim IW, Lee DS, Kang SH, Ahn ChW (2003) Thin Solid Films 441:115. doi:10.1016/S0040-6090(03)00909-X
4. Burn I (1971) Bull Am Ceram Soc 50:501
5. Puchmark C, Jiansirisomboon S, Rujijanagul G, Tunkasiri T (2004) Curr Appl Phys 4:179. doi:10.1016/j.cap.2003.11.003
6. Biggers JV, Schulze WA (1974) Bull Am Ceram Soc 53:809
7. Ishchuk VM, Baumer VN, Sobolev VL (2005) J Phys Condens Matter 17:L177. doi:10.1088/0953-8984/17/19/L01
8. Zhou L, Lupascu DC, Zimmermann A, Zhang Y (2005) J Appl Phys 97:124106. doi:10.1063/1.1946906
9. Ranjan R, Pandey D (2001) J Phys Condens Matter 13:4239. doi:10.1088/0953-8984/13/19/305
10. Pokharel BP, Pandey D (2000) J Appl Phys 88:5364. doi:10.1063/1.1317241
11. Xu Y, Singh RN (2000) J Appl Phys 88:7249. doi:10.1063/1.1325380
12. Bharadwaja SSN, Krupanidhi SB (2001) J Appl Phys 89:4541. doi:10.1063/1.1331659
13. Xu Y (1991) Ferroelectric materials and their applications. Elsevier Science Publishers BV, The Netherlands
14. Dai X, DiGiovanni A, Viehland D (1993) J Appl Phys 74:3399. doi:10.1063/1.354567
15. Thomas NW (1990) J Phys Chem Solids 51:1419. doi:10.1016/0022-3697(90)90025-B
16. Kong LB, Ma J (2002) Mater Lett 56:30. doi:10.1016/S0167-577X(02)00412-3
17. Landolt-Bornstein (1981) Numerical data and functional relationships in science and technology, vol 16. Springer-Verlag, Berlin, Heidelberg, New York